Neuroscience 127 (2004) 69–80

DENDRITIC SPINES DISAPPEAR WITH CHILLING BUT PROLIFERATE EXCESSIVELY UPON REWARMING OF MATURE HIPPOCAMPUS

S. A. KIROV,[a,c]* L. J. PETRAK,[d1] J. C. FIALA[d] AND K. M. HARRIS[b,c]

[a]*Department of Neurosurgery, Human Brain Laboratory, Medical College of Georgia, 1120 15th Street, CB-2607, Augusta, GA 30912, USA*

[b]*Department of Neurology, Medical College of Georgia, Augusta, GA 30912, USA*

[c]*Program in Synapses and Cell Signaling, Medical College of Georgia, Augusta, GA 30912, USA*

[d]*Department of Biology, Boston University, Boston, MA 02215, USA*

Abstract—More dendritic spine synapses occur on mature neurons in hippocampal slices by 2 h of incubation *in vitro*, than in perfusion-fixed hippocampus. What conditions initiate this spinogenesis and how rapidly do the spines begin to proliferate on mature neurons? To address these questions, CA1 field of the hippocampus neurons expressing green fluorescent protein in living slices from mature mice were imaged with two-photon microscopy. Spines disappeared and dendrites were varicose immediately after slice preparation in ice-cold artificial cerebrospinal fluid (ACSF). Electron microscopy (EM) revealed disrupted dendritic cytoplasm, enlarged or free-floating postsynaptic densities, and excessive axonal endocytosis. Upon warming dendritic varicosities shrank and spines rapidly reappeared within a few minutes illustrating the remarkable resilience of mature hippocampal neurons in slices. When membrane impermeant sucrose was substituted for NaCl in ACSF dendrites remained spiny at ice-cold temperatures and EM revealed less disruption. Nevertheless, spine number and length increased within 30 min in warm ACSF even when the extracellular calcium concentration was zero and synaptic transmission was blocked. When slices were first recovered for several hours and then chilled in 6 °C ACSF many spines disappeared and the dendrites became varicose. Upon re-warming varicosities shrank and spines reemerged in the same position from which they disappeared. In addition, new spines formed and spines were longer suggesting that chilling, not the initial injury from slicing, caused the spines to disappear while re-warming triggered the spine proliferation on mature neurons. The new spines might be a substrate for neuronal recovery of function, when neurons have been chilled or exposed to other traumatic conditions that disrupt ionic homeostasis.

Key words: synaptogenesis, structural plasticity, mature pyramidal CA1 neurons, cold, two-photon microscopy.

Hippocampal slices have become one of the most important model systems in which to study synaptic function and plasticity. In slices, as in the intact brain, dendritic spines are the primary location of excitatory synapses (Gray, 1959; Sorra and Harris, 1998). Whether new spines form or existing spines remodel remains an important open question especially for mature neurons (Harris and Kater, 1994). Studies show that normal synaptic plasticity, such as long-term potentiation, produces little or no net change in total spine or synapse number especially in the mature brain (Chang and Greenough, 1982; Desmond and Levy, 1990; Sorra and Harris, 1998; Geinisman, 2000) while abnormal epileptic activity causes substantial spine loss (Swann et al., 2000). In contrast there is a remarkable 40–50% increase in dendritic spine and synapse number in mature hippocampal slices relative to perfusion fixed hippocampus (Kirov et al., 1999). The increase in spine synapses stabilizes by 2 h and remains for at least 13 h *in vitro*. The time during recovery from slice preparation provides a unique opportunity to investigate mechanisms of spine proliferation on mature neurons.

There is a period lasting about 1 h after slice preparation during which synaptic responses are absent or markedly reduced (Schurr et al., 1984; Kirov et al., 1999). If synaptic transmission is blocked during slice preparation and incubation then more spines are produced than in active slices (Kirov and Harris, 1999). Together these findings suggested that spine proliferation might be initiated by the reduced synaptic activity (Kirov and Harris, 1999). However, more coated vesicles occur in presynaptic axons immediately after preparation of slices in immature (postnatal day 21) rats (Fiala et al., 2003). This observation implies an elevated release of glutamate from synaptic vesicles (Cremona and De Camilli, 1997) during the ischemic insult of slice preparation (Lipton, 1999). Similar events in the mature slices might trigger spinogenesis. Unlike mature hippocampal slices (Wenzel et al., 1994; Kirov et al., 1999), synapse number remains constant during the first 3 h of incubation in the immature slices (Fiala et al., 2003). Thus, widespread release of glutamate does not necessarily trigger an immediate synaptogenesis.

The drop in temperature, ATP, and glycogen during slice preparation changes ionic composition and intracellular H_2O and affects the basic biophysical properties of the neurons (Lipton, 1988; Siklos et al., 1997; Attwell and Laughlin, 2001; Volgushev et al., 2000a,b). Cold temperature also reduces spine and synapse number in the hip-

[1] Present address: Department of Cell Biology, Harvard Medical School, Boston, MA 02115, USA.

*Correspondence to: S. A. Kirov, Department of Neurosurgery, Medical College of Georgia, 1120 15th Street, CB-2607, Augusta, GA 30912, USA. Tel: +1-706-721-6051; fax: +1-706-721-6052.
E-mail address: skirov@mail.mcg.edu (S. A. Kirov).

Abbreviations: ACSF, artificial cerebrospinal fluid; AMPA, α-amino-3-hydroxy-5-methyl-4-isoxazole-proprionic acid; ANOVA, analysis of variance; APV, D(−)-2-amino-5-phosphonovaleric acid; CNQX, 6-cyano-7-nitroquinoxaline-2,3-dione; EM, electron microscopy; fEPSPs, field excitatory postsynaptic potentials; GFP, green fluorescent protein; GluR, glutamate receptor; Na^+-K^+-ATPase, sodium-potassium ion pump; PSDs, postsynaptic densities; TTX, tetrodotoxin.

0306-4522/04$30.00+0.00 © 2004 IBRO. Published by Elsevier Ltd. All rights reserved.
doi:10.1016/j.neuroscience.2004.04.053

pocampus of hibernating ground squirrels (Popov et al., 1992; Popov and Bocharova, 1992), however, within 2 h of arousal spine number increases beyond that found in active normothermic animals, suggesting that re-warming triggers spine proliferation. Functional consolidation of the spine synapses appears to take longer because hippocampal-dependent memory performance is reduced immediately after hibernation (Millesi et al., 2001). Similarly, cognitive decline occurs in human patients who have undergone hypothermic cardiopulmonary bypass during cardiac surgery (Newman et al., 2001) and after accidental deep hypothermia (Walpoth et al., 1997). Here two-photon and electron microscopy (EM) reveals dramatic changes in spine number on mature hippocampal dendrites with alterations in temperature and ionic conditions.

EXPERIMENTAL PROCEDURES

Hippocampal slice preparation and solutions

Brain slices (500 μm) were made from mature male mice of the B6.Cg-TgN(thy1-GFP [green fluorescent protein])MJrc strain (Feng et al., 2000) at postnatal days 51–135 according to standard protocols (Fiala et al., 2003). All procedures follow National Institutes of Health guidelines for the humane care and use of laboratory animals and underwent yearly review by the Animal Care and Use Committee at Boston University and subsequently at the Medical College of Georgia. All efforts were made to minimize animal suffering and to reduce the number of animals used. In total, 61 slices from 43 mice were used for these studies. Slices were prepared using two types of artificial cerebrospinal fluid (ACSF). The standard ACSF, contained 120 mM NaCl, 2.5 mM KCl, 25 mM $NaHCO_3$, 1 mM NaH_2PO_4, 2.5 mM $CaCl_2$, 1.3 mM $MgSO_4$ and 10 mM glucose, pH 7.4, osmolality 290 Mosm/kg H_2O. The Sucrose-ACSF was exactly the same except that it had 210 mM sucrose substituted for NaCl. When indicated the nominally Ca^{2+} free ACSF or Sucrose-ACSF contained 0 mM Ca^{2+} and 8 mM Mg^{2+}. Also as noted in some experiments ACSF had the sodium channel blocker tetrodotoxin (TTX; 1 μM), the *N*-methyl-D-aspartate glutamate receptor antagonist D(−)-2-amino-5-phosphonovaleric acid (APV; 50 μM) and α-amino-3-hydroxy-5-methyl-4-isoxazole-proprionic acid (AMPA) glutamate receptor antagonist 6-cyano-7-nitroquinoxaline-2,3-dione (CNQX; 20 μM). TTX was acquired from Calbiochem (La Jolla, CA, USA). All other drugs and chemicals were from Sigma Chemical (St. Louis, MO, USA). All drugs were prepared at 1000× concentration in stock solutions.

Mice were deeply anesthetized with halothane and decapitated. The head was immediately submerged into ACSF or Sucrose-ACSF ice slush bubbled with 95% O_2–5% CO_2. The brain was removed into the slush and the dorsal surface of one hemisphere was cut at a 60° angle from the horizontal plane and mounted ventral-side up on the cutting platform of a vibrating-blade microtome (VT1000S; Leica Instruments, Nussloch, Germany) and submerged in ACSF or Sucrose-ACSF oxygenated ice slush. Transverse slices including hippocampus, subiculum and cortex were cut from the middle third of the brain. The first slice was immediately placed into a submersion-type imaging chamber (RC-26GLP; Warner Instruments, Hamden, CT, USA) and perfused with oxygenated cold ACSF of the same composition that was used for cutting, at a flow rate of 8 ml/min by a peristaltic pump (Watson-Marlow, Wilmington, MA, USA) at indicated temperatures. The slice is held down by a custom made silver anchor of a "U" shape with a porous Millicell-CM membrane (Millipore, Bedford, MA, USA) (Potter, 2000. The average delay between animal death and placing the first slice into the imaging chamber was about 12 min. The remaining slices were transferred immediately after sectioning into an incubation chamber and placed onto nets glued to the stainless steel rings positioned over wells containing ACSF, and maintained at the interface of humidified 95% O_2–5% CO_2 atmosphere at 32 °C (pH 7.4). After at least 1.5 h of incubation a single ring with a slice, which stayed adhered to the net, was transferred into the imaging chamber. Temperature was monitored by a thermistor probe within 1 mm of a slice and was controlled by a bipolar temperature controller (Warner Instruments). When testing for the effects of cold temperature two temperature ranges were used, 5–7 °C and 13–17 °C, with the precise temperature for each experiment given in the results and figure legends.

Two-photon microscopy and electrophysiology

An imaging chamber was mounted on a fixed stage of the upright Axioscop II FS microscope (Carl Zeiss, Jena, Germany). Imaging was done at excitation wavelength 870 nm by two-photon microscopy using the Zeiss LSM 510 NLO multiphoton system directly coupled with the Spectra-Physics (Mountain View, CA, USA) Tsunami/5 W Millennia system. Three-dimensional time-lapse images were taken at 0.5 μm increments with a 63×/0.9 NA water-immersion objective (Carl Zeiss) using 4× magnification optical zoom, resulting in a nominal spatial resolution of 28 pixels/μm (12 bits per pixel, 2.24 μs pixel time). Emitted light was detected by LSM 510 NLO scan module with a pinhole entirely opened and data acquisition was controlled by Zeiss LSM 510 software. As configured for these experiments by utilizing the full width at half maximum of a point spread function measured with subresolution beads the microscope has the resolution of 0.380 μm in the lateral dimension and 1.950 μm in the axial dimension. To confirm slice viability the field excitatory postsynaptic potentials (fEPSPs) were recorded in the middle of *s. radiatum* using the Axopatch 200 amplifier (Axon Instruments, Foster City, CA, USA). Signals were filtered at 2 kHz, digitized at 10 kHz with Digidata 1200 D/A interface board (Axon Instruments) and analyzed with pClamp 8 software (Axon Instruments). The slope function (mV/ms) of the fEPSP was measured from the steepest 1 ms segment of the negative field potential over a series of stimulus intensities.

Dendrite analyses from two-photon microscopy

All analyses were done blind as to experimental conditions. The Zeiss LSM 510 image examiner was used with the Bitplane (Zurich, Switzerland) Imaris image visualization software to compare images of dendrites. The Scientific Volume Imaging (Hilversum, Netherlands) Huygens Professional image deconvolution software was used to process images before obtaining spine counts.

Electron microscopy and image analysis

One set of slices was prepared with ice-cold Sucrose-ACSF with 0 mM Ca^{2+} and 8 mM Mg^{2+} and imaged in the same media at 6 °C with two-photon microscopy. Then the slices were immersed in mixed aldehydes (6% glutaraldehyde, 2% paraformaldehyde, 1 mM $CaCl_2$, and 2 mM $MgCl_2$, in 0.1 M cacodylate buffer at pH 7.4) and exposed for 8 s to microwave irradiation for rapid fixation. Another set of slices was imaged in Sucrose-ACSF at 6 °C with 0 mM Ca^{2+} and 8 mM Mg^{2+} and then exposed to the standard ACSF at 6 °C until dendritic beading was observed. Then these slices were rapidly fixed and processed for EM. Standard microwave-enhanced procedures were used to process the slices through osmium, uranyl acetate, dehydration and embedding in resin (Fiala et al., 1998; Kirov et al., 1999).

Six slices in each of the two conditions were obtained from three animals. Five fields were photographed in each slice (total 30 fields) in the middle of *s. radiatum* at 6000× magnification on the JEOL 2010 electron microscope (JEOL, Peabody, MA, USA).

The images were randomized, coded and analyzed blind as to condition using IGL Trace software (http://synapses.mcg.edu/tools/) as previously described (Fiala et al., 2003). Each image provided about 175 μm^2 (2625 μm^2 in total per condition) to evaluate dendrite swelling, microtubule disassembly, free postsynaptic densities (PSDs), and coated vesicles in axons. Each dendritic profile was scored as having a sign of swelling if the cytoplasm was electron lucent, organelles were obviously swollen, or the plasma membrane had breaks. Microtubules and free PSDs were counted in cross-sectioned dendrites and their relative frequencies computed by dividing by dendritic profile area exclusive of spines. Coated vesicles and coated pits were counted and their frequencies were computed per unit area of analysis.

Statistical analysis

SigmaStat (Jandel, San Rafael, CA, USA) was used to compute paired *t*-test and Mann-Whitney rank sum test and repeated measurements analysis of variance (ANOVA). A two-way ANOVA, followed by Tukey's post hoc method, was used to evaluate what part of the variance between data arose from different experimental conditions and what part was due to differences between slices and animals. The significance criterion was set at $P<0.05$. Data are presented as mean±S.E.M. Time is given as mean±S.D.

RESULTS

Dendritic beading and spine loss during slice preparation

In the first set of experiments five hippocampal slices from five animals were prepared by vibroslicing one brain hemisphere under ice-cold conditions in ACSF according to standard protocols (see Experimental Procedures). These slices were imaged immediately with two-photon microscopy in cold (13.5±1.9 °C) ACSF. The dendrites of neurons imaged at 100–200 μm from the surface were found to be varicose and spine-free in all of the slices (Fig. 1A and 1B). This formation of varicosities along a dendrite is referred to as "dendritic beading" (Swann et al., 2000).

One important mechanism likely to contribute to the dendritic beading and spine loss during slice preparation is disrupted ionic and osmotic homeostasis involving elevated $[Na^+]_i$ and $[Cl^-]_i$ and the obligatory redistribution of H_2O when slices are prepared (Rothman, 1985; Strange, 1993; Siklos et al., 1997; Al-Noori and Swann, 2000; Oliva et al., 2002). To test this hypothesis another set of four slices from three animals was prepared in a modified ice-cold ACSF with plasma membrane impermeant sucrose substituted for NaCl (Sucrose-ACSF). Under these conditions, dendrites retained a spiny structure in all slices (Fig. 1C). The same dendrites became beaded and spine-free within 6±3 min of exposure to cold (6 °C) standard ACSF (Fig. 1D) suggesting that dendritic beading and spine loss involves accumulation of $[Na^+]_i$ and $[Cl^-]_i$ and the obligatory redistribution of H_2O.

Next, two experiments were conducted to determine whether the dendritic beading and spine loss during slice preparation might be due to Ca^{2+} and glutamate mediated excitotoxicity. First, four slices from four animals were prepared in ice-cold Sucrose-ACSF, this time containing 0 mM Ca^{2+} and 8 mM Mg^{2+}. The dendrites remained spiny under these conditions. However, when the same slices were exposed to cold (13.2±2.5 °C) standard ACSF containing 0 mM Ca^{2+} and 8 mM Mg^{2+}, dendritic beading and spine loss both occurred in all slices (Fig. 1E). These results suggest that the dendritic changes did not result from excessive influx of extracellular Ca^{2+}. In another experiment, we tested whether dendritic beading and spine loss during slice preparation required activation of glutamate receptors. Three slices from three animals were prepared in ice-cold Sucrose-ACSF containing 0 mM Ca^{2+} and 8 mM Mg^2 and exposed to cold (6.3±0.3 °C) ACSF containing APV, CNQX and TTX. In all slices the dendrites became beaded and spines were lost during 6.3±2.3 min of cold exposure suggesting that excessive activation of glutamate receptors is not the mechanism of dendritic beading and spine loss (Fig. 1F).

Upon warming dendrites recovered their normal spiny structure. All dendrites in five slices from five animals prepared with ice-cold ACSF lost their varicosities and reacquired dendritic spines at 32 °C in ACSF (Fig. 1G). In fact, the dendritic spines reappeared very rapidly, within 4.5±2 min ($n=4$ slices from four animals; Fig. 1H). Dendritic recovery did not require extracellular Ca^{2+} and was also within the 2.8±0.3 min time frame ($n=3$ slices from three animals). If, however, the slices ($n=6$ from four animals) were maintained in standard ACSF for 102±54 min at temperatures 5.3±1.8 °C, then the fEPSPs were absent and the dendrites were beaded even after 1 h of recovery at 32 °C in ACSF. fEPSPs were also absent following 1 h recovery at 32 °C in the standard ACSF if after preparation slices ($n=3$ from three animals) were exposed to cold 4.2±1.8 °C Sucrose-ACSF for 106±15 min but the dendrites were spiny. Thus, fEPSPs could be lost whether or not spines were lost.

Structural changes that were first observed on living dendrites with two-photon microscopy were supported by EM analyses from six slices from three animals (see Experimental Procedures). Slices prepared with ice-cold Sucrose-ACSF containing 0 mM Ca^{2+} and 8 mM Mg^{2+} had healthy dendrites with well-preserved dendritic spines and synapses, intact cytoplasm and uniformly spaced microtubules (Fig. 2A). In contrast, if slices were then exposed to standard ACSF at 6 °C dendrites showed signs of dendritic beading as evidenced by watery cytoplasm and thin cytoplasmic rims, swollen intracellular organelles and a lower density of microtubules (Fig. 2B). The percent of dendritic profiles with signs of swelling was 8.4±2.4 in the cold (6 °C) Sucrose-ACSF. In contrast 39.4±5.2% of dendritic profiles showed signs of swelling in slices subsequently exposed to cold (6 °C) ACSF ($P<0.001$, Fig. 2C). Microtubule density was 26.8±1.1 per 1 μm^2 in the slices in cold Sucrose-ACSF, whereas it was reduced to 16.6±1.1 per 1 μm^2 in cold ACSF ($P<0.001$, Fig. 2C).

Slices prepared with ice-cold Sucrose-ACSF containing 0 mM Ca^{2+} and 8 mM Mg^{2+} had compact PSDs and evenly distributed round smooth vesicles in their presynaptic axonal varicosities (Fig. 2A). In contrast slices exposed to ACSF at 6 °C exhibited enlarged PSDs and structures similar to PSDs were floating freely in the dendritic cytoplasm suggesting that some of the synapses were lost (Fig. 3A). The number of free PSD-like structures

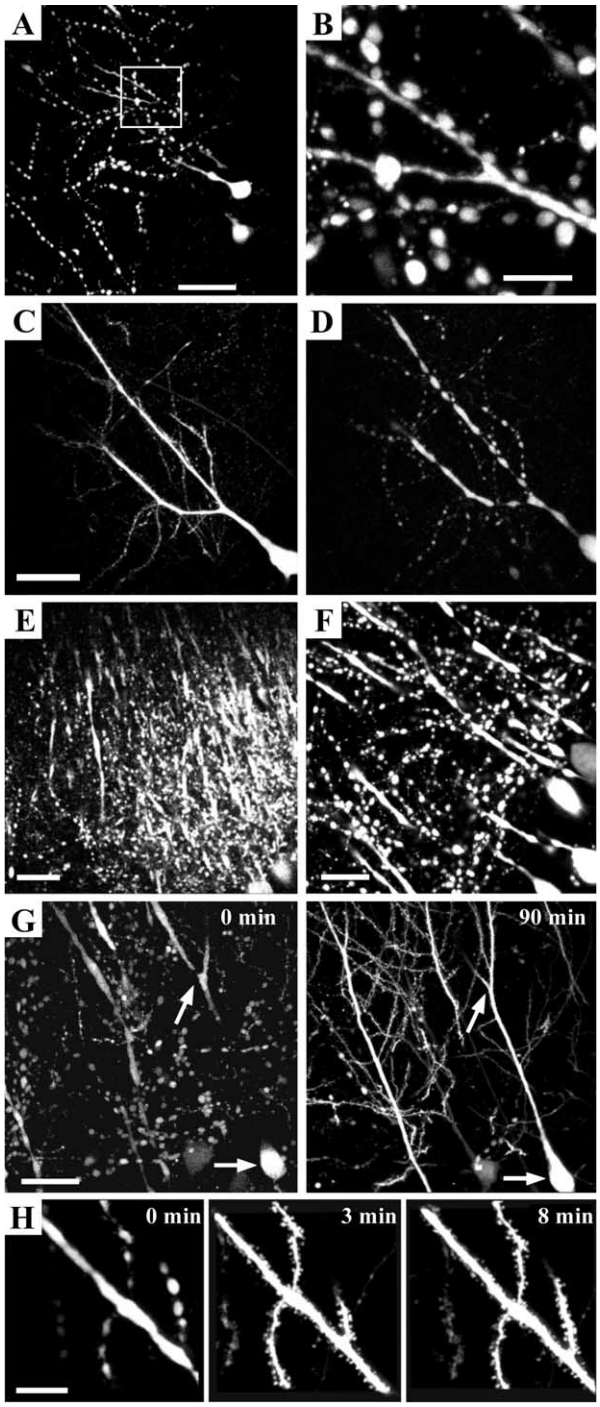

Fig. 1. Dendritic beading and spine loss during exposure to cold ACSF. (A) CA1 pyramidal cells in hippocampal slice prepared with ice-cold ACSF imaged 5 min later at 15 °C. Scale bar=40 μm. (B) Higher magnification of boxed region in (A). Scale bar=10 μm. (C) Spiny dendritic structure retained in slice prepared in ice-cold Sucrose-ACSF and imaged 5 min later at 6 °C. Scale bar=30 μm. (D) The same dendrites became beaded and spine-free after 5 min exposure to ACSF at 6 °C. (E) Beaded and spine-free CA1 dendrites in a slice prepared in ice-cold Sucrose-ACSF with 0 mM Ca^{2+} and 8 mM Mg^{2+} and then exposed to nominally Ca^{2+} free ACSF at 13 °C for 12 min. Scale bar=30 μm. (F) Beaded and spine-free dendrites in a slice prepared with ice-cold Sucrose-ACSF containing 0 mM Ca^{2+} and 8 mM Mg^{2+} and then exposed for 5 min to cold (7 °C) ACSF with ionotropic glutamate receptors antagonists and the sodium channel blocker, TTX. Scale bar=30 μm. (G) Recovery of dendrite structure with warming. Image acquired at 0 min in ACSF at 17 °C immediately after preparation in ice-cold ACSF and 90 min later upon recovery in ACSF at 32 °C. Arrows indicate the same structures before and after recovery. Scale bar=30 μm. (H) Rapid recovery of spines. Slice was prepared with ice-cold ACSF and the 0 min time point was obtained immediately at 17 °C. Subsequent images were taken in warm (32 °C) ACSF at 3 and 8 min later. Scale bar=10 μm.

per 1 μm^2 was only 0.7±0.5 in the slices in cold (6 °C) Sucrose-ACSF, which was much lower than 9.2±3 free PSD-like structures per 1 μm^2 in cold (6 °C) ACSF ($P<0.02$, Fig. 3B). In addition there were more coated vesicles and pits in axons after exposure to cold (6 °C) ACSF (Fig. 3C), suggesting vesicular release. The number of coated vesicles per 100 μm^2 was 23.4±1.5 in cold Sucrose-ACSF and 44.1±3.3 in cold ACSF ($P<0.001$, Fig. 3D). Thus EM confirmed that dendritic beading and spine loss was associated with substantial ultrastructural changes in dendritic cytoplasm, not a redistribution of GFP.

Spinogenesis following slice preparation

These findings motivated a series of quantitative experiments in an effort to answer the question when are the excess spines first formed in slices *in vitro* (Kirov et al., 1999). Since it was not feasible to answer this question in slices prepared in ice-cold standard ACSF, because the complete loss of dendritic spines under these conditions, the slices were first prepared with ice-cold Sucrose-ACSF containing 0 mM Ca^{2+} and 8 mM $Mg^{2+}$and then imaged immediately at 17 °C in the same medium. Under these conditions dendrites remained spiny (Fig. 4A). Furthermore, if these slices were maintained at 17 °C for up to 45 min spine number did not change. However, numerous new dendritic spines were formed if these slices were exposed to ACSF at 32 °C and re-imaged at approximately 30 min and 2 h during recovery (Fig. 4B). Dendrites with a diameter less than 1 μm were used to compute spine density to minimize the effect of the dendritic shaft obscuring spines. All dendritic protrusions were visualized through z-series and marked and counted as “spines” even though some may have been nonsynaptic filopodia (Ziv and Smith, 1996; Fiala et al., 1998). The length of the dendritic segment was measured and the number of spines per unit length was computed. The relative spine density increased by 31±5% during the first 36 min and up to 46±6% during 2 h of incubation in ACSF at 32 °C ($P<0.001$; Fig. 4C). Thin dendrites with diameters averaging 0.65±0.04 μm were utilized to compute changes in the relative spine lengths which were measured from the origin to the tip. Average spine length increased by 31±12% during the first half hour and by 37±7% during 2 h of recovery in ACSF at 32 °C ($P<0.001$; Fig. 4D). These results confirm our earlier findings in rat hippocampal slices (Kirov et al., 1999) and suggest that the new spines had begun to emerge on mature dendrites within 30 min *in vitro*.

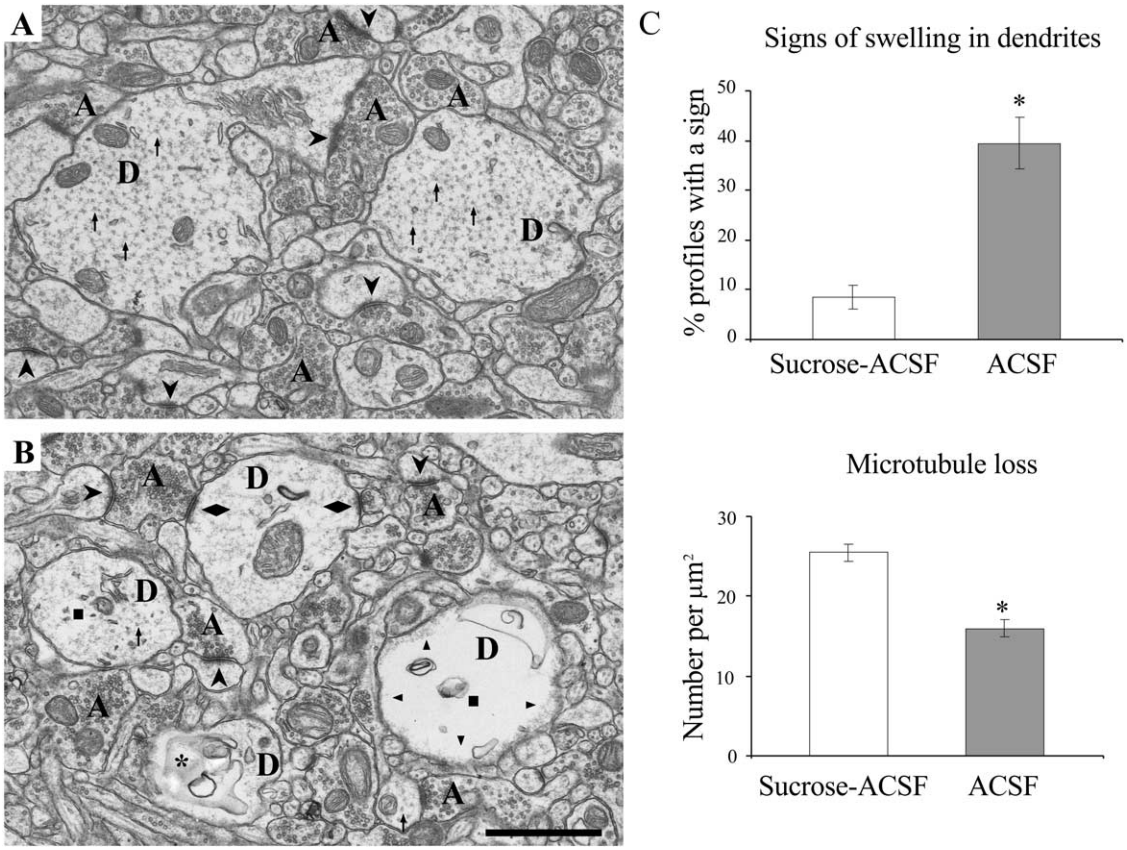

Fig. 2. Ultrastructural components of altered dendritic structure. Thirty fields in six slices from three animals were quantified. (A) Morphologically healthy neuropil in slices that were fixed after imaging for 16±5 min in (6 °C) Sucrose-ACSF after preparation in ice-cold Sucrose-ACSF containing 0 mM Ca^{2+} and 8 mM Mg^{2+}. Dendrites [D] have intact cytoplasm with a dense array of microtubules (arrows). Spines with healthy synapses (chevrons) appose axonal boutons [A] filled with synaptic vesicles. (B) Disrupted neuropil in slices that were prepared in ice-cold Sucrose-ACSF containing 0 mM Ca^{2+} and 8 mM Mg^{2+} and subsequently imaged while being exposed to ACSF at 6 °C for 16±1 min. Swollen dendrites [D] had watery cytoplasm with holes (squares), thin cytoplasmic rims (arrowheads), swollen organelles (asterisk) and few microtubules (arrows). Some swollen dendrites had enlarged synaptic contacts (diamonds). Some spines were present with synapses (chevrons) and axonal boutons [A] contained synaptic vesicles. Scale bar=1 μm. (C) The number of dendrites with signs of swelling increased and microtubules were lost after exposure of slices to ACSF at 6 °C (see Experimental Procedures). Asterisks indicate significant difference from Sucrose-ACSF condition (* $P<0.001$).

Spinogenesis was also imaged and quantified under conditions of blocked synaptic transmission. Slices were prepared in ice-cold Sucrose-ACSF with 0 mM Ca^{2+} and 8 mM $Mg^{2+}$and then imaged immediately at 17 °C in the same medium (Fig. 5A). The same dendrites were re-imaged at approximately 30 min and 2 h after exposure to the warm (32 °C) ACSF containing 0 mM Ca^{2+} and 8 mM Mg^{2+} and APV, CNQX and TTX (Fig. 5B). Dendrites with a diameter less than 1 μm were visualized in z-series. The relative spine density increased by 19±4% during the first 28 min and up to 35±8% during 2 h of incubation in blocking medium at 32 °C ($P<0.001$; Fig. 5C). There were no significant differences in the relative spine density between dendrites incubated in the standard ACSF and the blocking medium during the first 30 min or 2 h of incubation at 32 °C ($P=1.0$; compare Figs. 4C and 5C). Thin dendrites with a mean diameter of 0.41±0.02 μm were used to calculate the relative spine lengths. Average spine length increased by 23±5% during the first 30 min and by 27±4% during 2 h of incubation in the blocking medium at 32 °C ($P<0.001$; Fig. 5D). Compared with incubation in standard ACSF, spines were on average shorter during 30 min ($P<0.02$) and 2 h of incubation ($P<0.005$) in the blocking medium (compare Fig. 4D and 5D). These results suggest that the new spines start to form on mature dendrites within 30 min of incubation *in vitro* independent of the level of synaptic transmission.

Dendritic beading and spine loss in recovered slices

Experiments were designed to test the hypothesis that cold temperature was responsible for the dendritic beading and spine loss by using recovered slices to distinguish from the possible early effects of damage during slice preparation. Slices were prepared in Sucrose-ACSF containing 0 mM Ca^{2+} and 8 mM Mg^{2+} and then recovered *in vitro* for several hours at 32 °C in ACSF. These slices were then exposed to cold 5.9±0.2 °C ACSF. In all slices dendrites became beaded and spines were lost after 18±11 min of exposure to the cold (Fig. 6A–C). These data show that

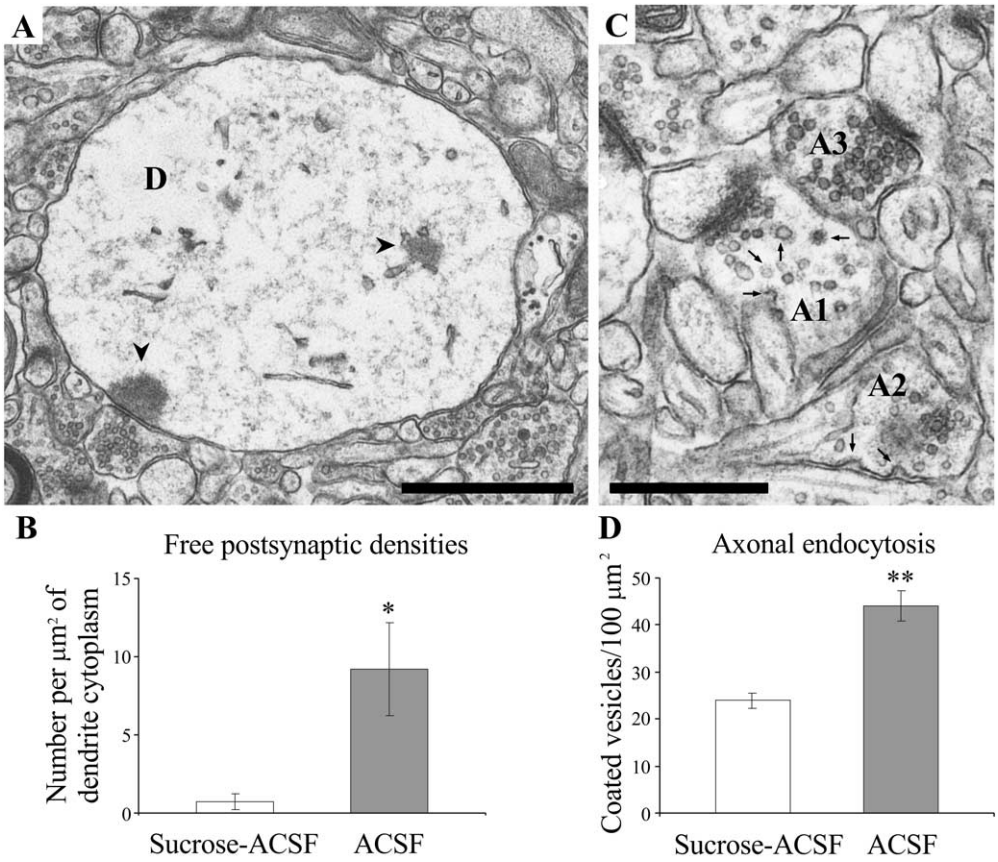

Fig. 3. Free PSD-like structures and axonal coated vesicles after exposure to cold (6 °C) ACSF. Thirty fields in six slices from three animals were quantified. (A) Dendrite [D] containing enlarged or free PSD-like structures (chevrons) when prepared in ice-cold Sucrose-ACSF containing 0 mM Ca^{2+} and 8 mM Mg^{2+} and subsequently exposed to 6 °C ACSF. Scale bar=1 μm. (B) More free PSDs in dendrites during 6 °C ACSF (* $P<0.02$). (C) Variation among axons in amount of endocytosis. Several coated vesicles (arrows) and relatively depleted synaptic vesicle number in one axonal bouton [A1]. Clathrin-coated pits (arrows) in another axonal bouton [A2]. A third axonal bouton [A3] shows no signs of clathrin-coated vesicles and has many synaptic vesicles. Scale bar=0.5 μm. (D) Mean increase in coated vesicles in axonal boutons after application of ACSF at 6 °C (** $P<0.001$).

dendritic beading and spine loss away from the cut surfaces was not due to the traumatic injury during slice preparation.

Another set of experiments was performed to determine whether the dendritic beading and spine loss in recovered slices exposed to cold was dependent on the extracellular concentration of Na^+ and Cl^- ions. Slices were prepared in Sucrose-ACSF containing 0 mM Ca^{2+} and 8 mM Mg^{2+} and then recovered *in vitro* for several hours at 32 °C in ACSF. Next three slices from two animals were exposed to Sucrose-ACSF at 6.6±0.4 °C for 40 min. In all slices dendritic beading did not occur and spines were not lost (Fig. 7A). When these three slices were subsequently exposed to standard ACSF at 6.8±0.6 °C, the dendrites became beaded and spines were lost in all slices during 6.3±1.5 min of cold exposure (Fig. 7B). These findings suggest that dendritic beading during intensive cold is dependent on the concentration of Na^+ and Cl^- ions.

The sodium-potassium ion pump (Na^+-K^+-ATPase) plays a vital role in neurons to maintain ionic and osmotic balance by creating Na^+ and K^+ electrochemical gradients across plasma membranes. Inhibition of the Na^+-K^+-ATPase might lead to dendrite and neuron swelling (Lowe, 1978; Basavappa et al., 1998; Buckley et al., 1999). To test this hypothesis, slices were first recovered *in vitro* for several hours in ACSF and then exposed to ouabain at 32 °C. The dendrites became beaded and spines were lost during 5 min exposure to ouabain and fEPSPs were lost as would be expected under these conditions (Obeidat et al., 2000; Fig. 8). These data suggest that the inhibition of the Na^+-K^+-ATPase may contribute to the dendritic beading and spine loss during slice preparation.

Spinogenesis in recovered slices

These experiments were designed to test whether warming after exposure to cold leads to spinogenesis. Fully recovered slices were used to eliminate the immediate synaptogenic response that might be a response to damage during slice preparation and thus not specific to temperature. Individual dendrites were imaged in recovered slices before (Fig. 9A), during (Fig. 9B), and after exposure to cold (5±0.5 °C) ACSF (Fig. 9C). Slice viability was confirmed by recording fEPSPs in response to constant stimulus intensity at the different temperatures (Fig. 9D).

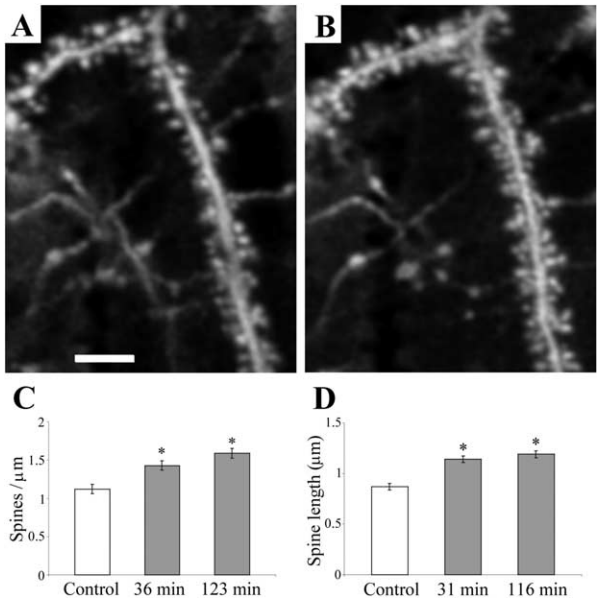

Fig. 4. Increase in spine frequency *in vitro*. Spinogenesis during *in vitro* recovery in ACSF. (A) Control dendrites in slice prepared with ice-cold Sucrose-ACSF with 0 mM Ca^{2+} and 8 mM Mg^{2+} and imaged immediately in cold (17 °C) Sucrose-ACSF with 0 mM Ca^{2+} and 8 mM Mg^{2+}. Scale bar=5 μm. (B) Spinier dendrites after 2 h of incubation in ACSF at 32 °C. (C) Spine density immediately after preparation (control), and 36±11 min and 123±21 min after exposure to the warm ACSF at 32 °C. Nineteen dendrites in five slices from five animals were quantified. Asterisks indicate significant differences from control (* $P<0.001$). Spine density also increased between 36 and 123 min ($P<0.005$). (D) Average spine length in control, 31±8 min and 116±25 min after exposure to the warm ACSF at 32 °C. For each time point, 130 spines were measured along five dendrites in five slices from five animals. Asterisks indicate significant differences from control (* $P<0.001$).

Slices were also tested with increasing stimulus intensities to generate an input-output curve (Fig. 9E). Slices had equal fEPSP slopes and stable baseline responses before and after recovery from exposure to cold ACSF ($P=0.4$; Fig. 9E). When exposed to cold ACSF for 20±13 min, dendrites became varicose and 37.8±13% of spines were lost under these conditions (six dendritic segments in five slices from five animals; Fig. 9B). Upon re-exposure to ACSF at 32 °C dendritic varicosities disappeared and all lost spines returned to the same location from which they disappeared. New spines formed and spine density increased above the original recovered density by 9±3% during the first 30 min of re-warming, and further by 12±2% during 83 min (10 dendritic segments in five slices from five animals; $P<0.001$; Fig. 9F). There were no significant differences in spine density between these two time points ($P=0.6$). Thin dendrites with diameter 0.48±0.02 μm were used to calculate the relative spine length in the recovered slices and during re-warming. Average spine length increased by 42±11% during the first 30 min and by 37±7% during 81 min of re-warming in ACSF at 32 °C ($P<0.001$; Fig. 9G). There were no differences in spine length between 30 min and 81 min of re-warming ($P=0.7$). Dendrites recovered *in vitro* have more synapses than dendrites in perfusion fixed hippocampus (Kirov et al., 1999). These observations suggest that events occurring during warming after exposure to the cold ACSF could be the trigger of spine proliferation.

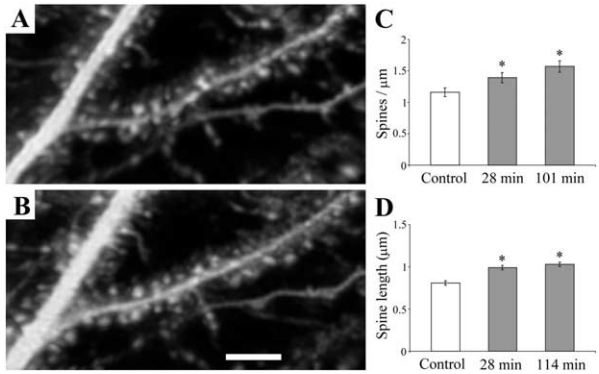

Fig. 5. Spinogenesis *in vitro* during blocked synaptic transmission. (A) Control dendrites in slice prepared in ice-cold Sucrose-ACSF with 0 mM Ca^{2+} and 8 mM Mg^{2+} and imaged immediately in cold (17 °C) Sucrose-ACSF with 0 mM Ca^{2+} and 8 mM Mg^{2+}. (B) Same dendrites as in A are spinier after 2 h 10 min of incubation in the warm (32 °C) ACSF with 0 mM Ca^{2+} and 8 mM Mg^{2+} and APV, CNQX and TTX. Scale bar=5 μm. (C) Increased spine density at 28±13 min and 101±19 min of incubation in the warm (32 °C) ACSF with 0 mM Ca^{2+} and 8 mM Mg^{2+} and activity antagonists. Thirteen dendrites in three slices from three animals were imaged. Asterisks indicate significant differences from control (* $P<0.001$). Spine density also increased between 28 and 101 min ($P<0.02$). (D) Increase in average spine length during 28±10 min and 114±17 min of warm (32 °C) incubation under conditions of blocked synaptic transmission. For each time point, 127 spines were measured along five dendrites in three slices from three animals. Asterisks indicate significant differences from control (* $P<0.001$).

DISCUSSION

These findings are the first to show rapid spine proliferation on mature dendrites within minutes of altering temperature. Live imaging revealed dendritic varicosities and loss of spines in ice-cold ACSF. Upon warming the varicosities disappeared, spines reemerged in the same location from which they disappeared, new spines formed, and spines elongated. When NaCl was replaced with sucrose during slice preparation, dendrites retained their spiny structure. However, more spines emerged and spines were longer during warming in either standard ACSF or when synaptic transmission was blocked. These findings illustrate the structural resiliency of mature neurons. The rapid recovery and subsequent stabilization *in vitro* of dendritic, spine, and synaptic structure affirms the validity of studying synaptic mechanisms in hippocampal slices (Kirov et al., 1999). New temperature dependent mechanisms of spine formation were also revealed during the rapid recovery of mature neurons in slices.

Resiliency of mature hippocampal neurons in slices

Dendritic spines reappeared quickly with more than half emerging during the first 30 min of incubation. Spine and synapse number on CA1 dendrites of mature pyramidal cells reached a plateau by 2 h and remained stable for at

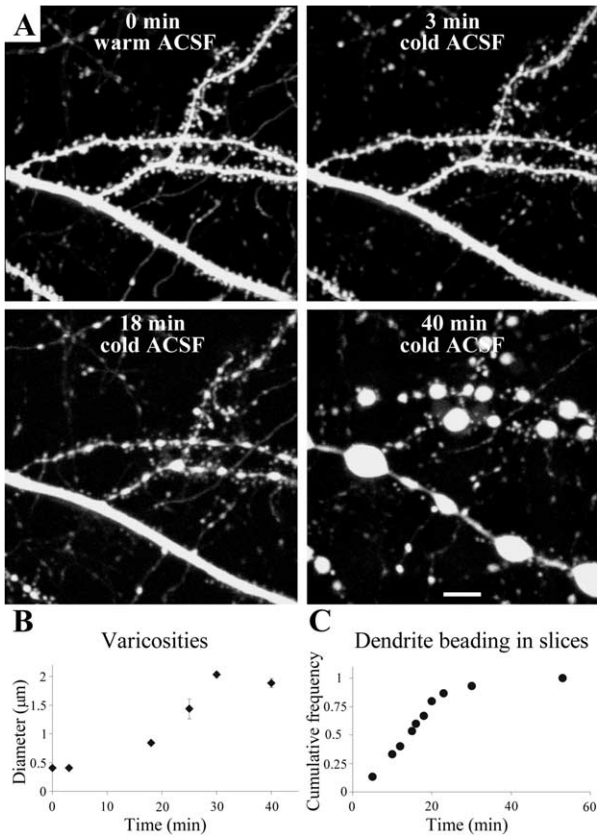

Fig. 6. Dendrites lose spines in cold ACSF. (A) Beading of CA1 dendrites in *s.radiatum* at 6 °C in the presence of NaCl; 0 min image of spiny recovered dendrites at 32 °C in ACSF. Subsequent time points during application of ACSF at 6 °C. Scale bar=5 μm. (B)Time course of dendritic beading presented in (A). For each thin dendrite the average diameter was measured at time 0 min. Varicosities were first detected by 18 min of exposure to cold and their average diameter was increased significantly during the next 12 min ($P<0.001$). (C)Cumulative relative frequency of the time when dendritic beading was first detected during exposure to cold 5.9±0.2 °C ACSF in 15 slices from 13 animals.

least 13 h *in vitro* (Kirov et al., 1999) clearly providing a long period during which synaptic mechanisms and plasticity can be investigated on healthy dendrites. What is not clear, however, is whether the re-emergent and new spines make synapses with the same or different presynaptic axons from those the dendrites made synapses with *in vivo* prior to slicing.

Several other transient changes accompany the resiliency of dendritic structure on mature hippocampal neurons in slices. There is a transient drop in ATP and glycogen that parallels the transient loss of synaptic transmission (Lipton and Whittingham, 1982; Schurr et al., 1984; Lipton, 1988, 1999; Kirov et al., 1999; Fiala et al., 2003). Dendritic microtubules depolymerize during slicing, but then begin to repolymerize within minutes and reach their full length within a few hours of warm incubation *in vitro* (Weisenberg and Deery, 1981; Burgoyne et al., 1982; Fiala et al., 2003). A transient elevation in the dendritic Ca^{2+} might cause this depolymerization because the normal compartmentalization of Ca^{2+} near the synapse would be

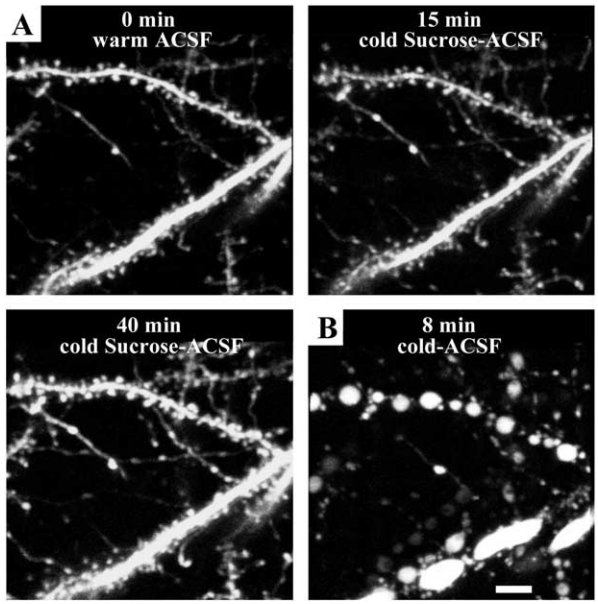

Fig. 7. Dendrites retain spines in cold Sucrose-ACSF. (A) Spiny recovered dendrites at 32 °C in ACSF (0 min image). Application of Sucrose-ACSF at 6 °C for 40 min did not result in spine loss or dendrite beading. (B) Subsequent exposure of the same dendrites to ACSF at 6 °C results in spine loss and dendrite beading. Scale bar=5 μm.

lost when spines are lost (Sabatini et al., 2001). EM reveals a transient increase in Ca^{2+}-containing precipitates within dendritic compartments immediately after hippocampal slice preparation (Siklos et al., 1997). There are also elevations in mRNA expression at the time of slicing including an increase in mRNAs for glutamate receptor

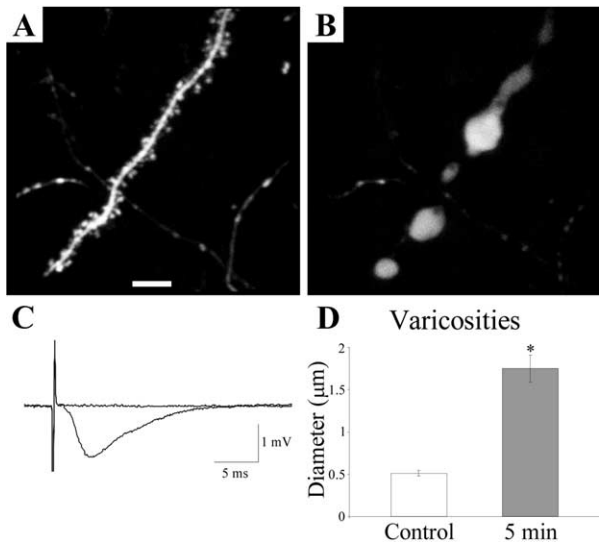

Fig. 8. Dendrite beading in ouabain. (A) Dendrite from slice recovered *in vitro* at 32 °C. (B) Same dendrite 5 min after application of 100 μM of ouabain in ACSF at 32 °C. Scale bar=5 μm. (C) Superimposed fEPSPs in control ACSF and after dendritic beading in ouabain. (D) Diameter of varicosities during 5 min of exposure to 100 μM of ouabain at 32 °C was significantly higher than dendritic diameter before ouabain application ($P<0.001$). Ten dendrites in four slices from three animals were imaged.

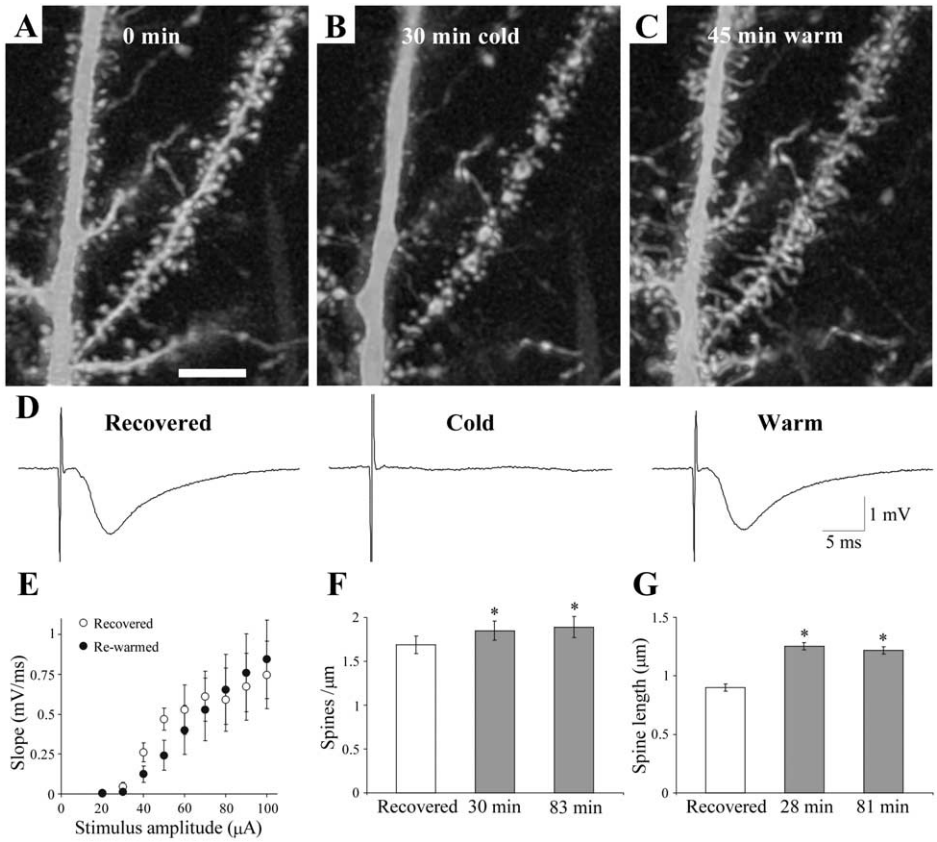

Fig. 9. Spine proliferation in recovered slices after exposure to cold ACSF. (A) Image of recovered apical and lateral dendrites of CA1 pyramidal cell in a slice incubated at 32 °C in ACSF for 150 min. Scale bar=5 μm. (B) Dendrite beading and spine loss after 30 min exposure to cold ACSF at 6 °C. (C) Spinogenesis and disappearance of dendrite varicosities after 45 min of re-exposure to 32 °C ACSF. (D) Corresponding physiological responses before and during exposure to cold and after re-warming. (E) Input-output function (mean±S.E.) in recovered slices before cold exposure and after responses stabilize during re-warming (n=5 slices from four animals). (F) Increase in spine density after re-warming relative to the recovered density. Ten dendritic segments were imaged in five slices from five animals. Recovered spine density was determined after 228±132 min of incubation in an interface chamber in ACSF at 32 °C. Slices were then exposed to ACSF at 5.5°±0.5 °C for 20±13 min until dendrites became varicose. Dendrites were analyzed at 30±3 min and 83±19 min after re-exposure to the warm media. Asterisk indicates significant difference from the recovered time point (* P<0.002). (G) Increase in average spine length during 28±5 min and 80±5 min of re-warming at 32 °C comparable to recovered dendrites imaged in slices incubated at 32 °C in ACSF for 191±113 min. For each time point 201 spines were measured on eight dendrites in five slices from five animals. Asterisks indicate significant differences from control (* P<0.001).

(GluR)1, GluR2 and GluR3 AMPA receptor subunits, transcription factors such as *c-fos*, *zif268* and CCAAT enhancer binding protein β and δ, and neurotrophin brain-derived neurotrophic factor (Zhou et al., 1995; Taubenfeld et al., 2002). In some cases induction of the mRNA results in a net increase in the corresponding protein (Zhou et al., 1995), while in others it does not (Taubenfeld et al., 2002), although there might be more degradation that would mask an increased protein synthesis. Thus, molecular mechanisms exist that could restore dendritic and synaptic structure rapidly *in vitro*.

Rapid disruption of dendritic structure in the cold

It is generally thought that hypothermia should minimize neuronal disruption (Newman et al., 1992); however, spine loss and dendritic beading occurred immediately after slice preparation in ice-cold ACSF suggesting that hypothermia does not protect dendritic structure. Dendritic beading and spine loss accompany hypoxia–ischemia *in vivo* or anoxia–hypoglycemia *in vitro* (Hsu and Buzsaki, 1993; Hasbani et al., 2001; Jourdain et al., 2002), traumatic head injury (Castejon, 1998) and epileptic seizures (Scheibel et al., 1974; Isokawa and Levesque, 1991). Under these circumstances the dendritic disruption has been attributed to Ca^{2+} and glutamate-mediated excitotoxicity because increased $[Ca^{2+}]_i$ depolymerizes the dendritic cytoskeleton (Halpain et al., 1998; Segal, 2001). Intense activation of glutamate receptors can also cause beading and spine loss independently of elevated $[Ca^{2+}]_i$ (Hasbani et al., 1998; Swann et al., 2000; Obeidat et al., 2000; Al-Noori and Swann, 2000; Oliva et al., 2002). Our experiments show, however, that beading and spine loss occur in the absence of $[Ca^{2+}]_o$ and glutamate receptor activation immediately after slice preparation. These findings suggest that mechanisms other than Ca^{2+} and glutamate-mediated excitotoxicity must be operating.

Another mechanism of dendritic beading could be the disruption of ionic and osmotic homeostasis resulting in the

influx of Na^+ and Cl^- accompanied by an obligatory uptake of H_2O (Strange, 1993; Hoffmann and Dunham, 1995; Siklos et al., 1997; Schwartzkroin et al., 1998; Swann et al., 2000). In support of this hypothesis we found that if NaCl was replaced with sucrose in the ACSF, the dendrites retained their spiny structure during exposure to cold. In further support were the experiments using ouabain to inhibit the Na^+-K^+-ATPase, which is vital in the control of ionic and osmotic homeostasis (Alberts et al., 1994; Hoffmann and Dunham, 1995). Application of ouabain resulted in dendritic beading on the recovered hippocampal neurons in warm ACSF. Similar dendritic beading occurs when cortical neurons are perfused with ouabain *in vivo* (Lowe, 1978). There are many downstream effects that could be triggered by disrupting Na^+ and K^+ gradients across plasma membranes either in the cold or by direct inhibition of the Na^+-K^+-ATPase. For example, the function of other membrane transporters involved in cell volume regulation will be disrupted. It was beyond the scope of this study to specify exactly which of these mechanisms are responsible for dendritic beading. However, disruption of ionic and osmotic homeostasis offers a rich array of alternative mechanisms to glutamate-mediated excitotoxicity.

Rapid recovery of dendritic structure

The recovery of dendritic and spine structure during re-warming after slice preparation was fast and occurred independently of $[Ca^{2+}]_o$. The shrinkage of the varicosities is consistent with the rapid recovery of osmotic homeostasis (Hoffmann and Dunham, 1995). The speed of spine recovery might suggest that the spines had merely retracted or had been overwhelmed by varicosities and then reappeared in their original locations when the varicosities shrank, as after a brief exposure to cold of recovered *in vitro* dendrites. However, following slice preparation EM analysis revealed abnormally thick PSDs on swollen dendritic varicosities as well as structures similar to PSDs floating freely in the dendritic cytoplasm (Dosemeci et al., 2000). These findings suggest that at least some synapses were disrupted and lost. In addition, the cytoskeleton in the swollen dendritic varicosities was forced to a thin rim surrounding a watery center. Moreover, in recovered slices the spines were longer upon re-warming. Unequivocal identification of spine type and whether or not they have synapses will require a serial EM analysis that is beyond the scope of this study. The imaging findings strongly suggest that recovery involves the formation of new spines in addition to reinstating previously existing spines on mature dendrites.

Spine proliferation after re-warming

Spine proliferation and synaptogenesis after re-warming extends beyond the CA1 pyramidal cell dendrites in slices (Kirov et al., 1999) occurring also on the soma of mature dentate granule cells (Wenzel et al., 1994) and on the CA3 pyramidal cells dendrites of ground squirrels after arousal from hibernation (Popov et al., 1992; Popov and Bocharova, 1992). How might new spines be triggered on mature neurons either after slice preparation or in recovered slices exposed to cold and then re-warmed? Spine outgrowth depends on an optimal increase in cytosolic Ca^{2+} (Segal, 2001). Here we demonstrated that spine proliferation occurs in the absence of $[Ca^{2+}]_o$ and also when glutamate receptors are blocked. Hence, release from intracellular stores must be sufficient to trigger spine proliferation. As discussed above, an elevation occurs in $[Na^+]_i$ during slicing and exposure to cold. This elevated Na^+ will activate the mitochondrial $2Na^+$-Ca^{2+} exchanger upon re-warming, and release Ca^{2+} from mitochondrial stores which in turn will initiate release of Ca^{2+} from smooth endoplasmic reticulum (Lipton, 1999; Sabatini et al., 2001). Hence, there is a route by which intracellular stores of Ca^{2+} can be accessed during slice recovery and which might induce spine proliferation. The preservation or elimination of spines on developing neurons depends on synaptic activity (Katz and Shatz, 1996). Blocking synaptic transmission during 8 h of slice incubation resulted in more spines on mature dendrites (Kirov and Harris, 1999) consistent with excess dendritic spines remaining while synaptic activity is low. How long they can remain without appropriate activation will require further experimentation.

Implications

There are several implications of these findings. Despite spine loss and dendritic disruption during slice preparation, mature hippocampal neurons are remarkably resilient and spines reappear within a few minutes *in vitro*. Thus, the recovered slice preparation is an excellent model in which to study synaptic plasticity. The findings also have important implications for understanding mechanisms of learning and memory. Hypothermia during hibernation reduces dendritic arborization of CA3 pyramidal cells, induces spine loss and could affect hippocampus dependent memory performance (Popov et al., 1992; Popov and Bocharova, 1992; Millesi et al., 2001). A loss of spines and synapses might contribute to the serious and enduring confusion that occurs in patients whose brains have been chilled or exposed to altered ionic conditions (Walpoth et al., 1997; Newman et al., 2001). Rapid spine proliferation could be a substrate for neuronal recovery of function after injury. If some re-emerging spines do not re-synapse with the same axons, however, it would explain the enduring loss of some memories while still providing a substrate to relearn.

Acknowledgements—We thank Dr. Joshua Sanes (Washington University, St. Louis, MO) for his generous gift of transgenic mice, Dr. Julia Fomitcheva (Medical College of Georgia, Augusta, GA) for critical reading of this manuscript and Ms Marcia Feinberg (Boston University, Boston, MA) for the technical assistance with electron microscopy. This research was supported by NIH KO1MH02000 and NS21184, NS33574 and the Packard Foundation.

REFERENCES

Alberts B, Bray D, Lewis J, Raff M, Roberts K, Watson J (1994) Molecular biology of the cell, 3rd ed. New York, New York: Garland Publishing.

Al-Noori S, Swann JW (2000) A role for sodium and chloride in kainic acid-induced beading of inhibitory interneuron dendrites. Neuroscience 101:337–348.

Attwell D, Laughlin SB (2001) An energy budget for signaling in the grey matter of the brain. J Cereb Blood Flow Metab 21:1133–1145.

Basavappa S, Mobasheri A, Errington R, Huang CC, Al-Adawi S, Ellory JC (1998) Inhibition of Na^+, K^+-ATPase activates swelling-induced taurine efflux in a human neuroblastoma cell line. J Cell Physiol 174:145–153.

Buckley DL, Bui JD, Phillips MI, Zelles T, Inglis BA, Plant HD, Blackband SJ (1999) The effect of ouabain on water diffusion in the rat hippocampal slice measured by high resolution NMR imaging. Magn Reson Med 41:137–142.

Burgoyne RD, Gray EG, Sullivan K, Barron J (1982) Depolymerization of dendritic microtubules following incubation of cortical slices. Neurosci Lett 31:81–85.

Castejon OJ (1998) Electron microscopic analysis of cortical biopsies in patients with traumatic brain injuries and dysfunction of neurobehavioural system. J Submicrosc Cytol Pathol 30:145–156.

Chang FL, Greenough WT (1982) Lateralized effects of monocular training on dendritic branching in adult split-brain rats. Brain Res 232:283–292.

Cremona O, De Camilli P (1997) Synaptic vesicle endocytosis. Curr Opin Neurobiol 7:323–330.

Desmond NL, Levy WB (1990) Morphological correlates of long-term potentiation imply the modification of existing synapses, not synaptogenesis, in the hippocampal dentate gyrus. Synapse 5:139–143.

Dosemeci A, Reese TS, Petersen J, Tao-Cheng JH (2000) A novel particulate form of $Ca^{(2+)}$/calmodulin-dependent [correction of $Ca^{(2+)}$/CaMKII-dependent] protein kinase II in neurons. J Neurosci 20:3076–3084.

Feng G, Mellor RH, Bernstein M, Keller-Peck C, Nguyen QT, Wallace M, Nerbonne JM, Lichtman JW, Sanes JR (2000) Imaging neuronal subsets in transgenic mice expressing multiple spectral variants of GFP. Neuron 28:41–51.

Fiala JC, Kirov SA, Feinberg MD, Petrak LJ, George P, Goddard CA, Harris KM (2003) Timing of neuronal and glial ultrastructure disruption during brain slice preparation and recovery in vitro. J Comp Neurol 465:90–103.

Fiala JC, Feinberg MD, Popov V, Harris KM (1998) Synaptogenesis via dendritic filopodia in developing hippocampal area CA1. J Neurosci 18:8900–8911.

Gray EG (1959) Axo-somatic and axo-dendritic synapses of the cerebral cortex: an electron microscopic study. J Anat 93:420–433.

Geinisman Y (2000) Structural synaptic modifications associated with hippocampal LTP and behavioral learning. Cereb Cortex 10:952–962.

Halpain S, Hipolito A, Saffer L (1998) Regulation of F-actin stability in dendritic spines by glutamate receptors and calcineurin. J Neurosci 18:9835–9844.

Harris KM, Kater SB (1994) Dendritic spines: cellular specializations imparting both stability and flexibility to synaptic function. Annu Rev Neurosci 17:341–371.

Hasbani MJ, Hyrc KL, Faddis BT, Romano C, Goldberg MP (1998) Distinct roles for sodium, chloride, and calcium in excitotoxic dendritic injury and recovery. Exp Neurol 154:241–258.

Hasbani MJ, Schlief ML, Fisher DA, Goldberg MP (2001) Dendritic spines lost during glutamate receptor activation reemerge at original sites of synaptic contact. J Neurosci 21:2393–2403.

Hoffmann EK, Dunham PB (1995) Membrane mechanisms and intracellular signalling in cell volume regulation. Int Rev Cytol 161:173–262.

Hsu M, Buzsaki G (1993) Vulnerability of mossy fiber targets in the rat hippocampus to forebrain ischemia. J Neurosci 13:3964–3979.

Isokawa M, Levesque MF (1991) Increased NMDA responses and dendritic degeneration in human epileptic hippocampal neurons in slices. Neurosci Lett 132:212–216.

Jourdain P, Nikonenko I, Alberi S, Muller D (2002) Remodeling of hippocampal synaptic networks by a brief anoxia-hypoglycemia. J Neurosci 22:3108–3116.

Katz LC, Shatz CJ (1996) Synaptic activity and the construction of cortical circuits. Science 274:1133–1138.

Kirov SA, Harris KM (1999) Dendrites are more spiny on mature hippocampal neurons when synapses are inactivated. Nat Neurosci 2:878–883.

Kirov SA, Sorra KE, Harris KM (1999) Slices have more synapses than perfusion-fixed hippocampus from both young and mature rats. J Neurosci 19:2876–2886.

Lipton P, Whittingham TS (1982) Reduced ATP concentration as a basis for synaptic transmission failure during hypoxia in the in vitro guinea-pig hippocampus. J Physiol 325:51–65.

Lipton P (1988) Regulation of glycogen in the dentate gyrus of the in vitro guinea pig hippocampus: effect of combined deprivation of glucose and oxygen. J Neurosci Methods 28:147–154.

Lipton P (1999) Ischemic cell death in brain neurons. Physiol Rev 70:1431–1568.

Lowe DA (1978) Morphological changes in the cat cerebral cortex produced by superfusion of ouabain. Brain Res 148:347–363.

Millesi E, Prossinger H, Dittami JP, Fieder M (2001) Hibernation effects on memory in European ground squirrels (*Spermophilus citellus*). J Biol Rhythms 16:264–271.

Newman GC, Qi H, Hospod FE, Grundmann K (1992) Preservation of hippocampal brain slices with in vivo or in vitro hypothermia. Brain Res 575:159–163.

Newman MF, Kirchner JL, Phillips-Bute B, Gaver V, Grocott H, Jones RH, Mark DB, Reves JG, Blumenthal JA (2001) Longitudinal assessment of neurocognitive function after coronary-artery bypass surgery. N Engl J Med 344:395–402.

Obeidat AS, Jarvis CR, Andrew RD (2000) Glutamate does not mediate acute neuronal damage after spreading depression induced by O_2/glucose deprivation in the hippocampal slice. J Cereb Blood Flow Metab 20:412–422.

Oliva AA Jr, Lam TT, Swann JW (2002) Distally directed dendrotoxicity induced by kainic acid in hippocampal interneurons of green fluorescent protein-expressing transgenic mice. J Neurosci 22:8052–8062.

Popov VI, Bocharova LS, Bragin AG (1992) Repeated changes of dendritic morphology in the hippocampus of ground squirrels in the course of hibernation. Neuroscience 48:45–51.

Popov VI, Bocharova LS (1992) Hibernation-induced structural changes in synaptic contacts between mossy fibres and hippocampal pyramidal neurons. Neuroscience 48:53–62.

Potter SM (2000) Two-photon microscopy for 4D imaging of living neurons. In: Imaging neurons: a laboratory manual (Yuste R, Lanni F, Konnerth A, eds), pp 20.1–20.16. Cold Spring Harbor, New York: Cold Spring Harbor Laboratory Press.

Rothman SM (1985) The neurotoxicity of excitatory amino acids is produced by passive chloride influx. J Neurosci 5:1483–1489.

Sabatini BL, Maravall M, Svoboda K (2001) $Ca^{(2+)}$ signaling in dendritic spines. Curr Opin Neurobiol 11:349–356.

Scheibel ME, Crandall PH, Scheibel AB (1974) The hippocampal-dentate complex in temporal lobe epilepsy: a Golgi study. Epilepsia 15:55–80.

Schurr A, Reid KH, Tseng MT, Edmonds HL Jr (1984) The stability of the hippocampal slice preparation: an electrophysiological and ultrastructural analysis. Brain Res 297:357–362.

Schwartzkroin PA, Baraban SC, Hochman DW (1998) Osmolarity, ionic flux, and changes in brain excitability. Epilepsy Res 32:275–285.

Segal M (2001) Rapid plasticity of dendritic spine: hints to possible functions? Prog Neurobiol 63:61–70.

Siklos L, Kuhnt U, Parducz A, Szerdahelyi P (1997) Intracellular calcium redistribution accompanies changes in total tissue Na^+, K^+ and water during the first two hours of in vitro incubation of hippocampal slices. Neuroscience 79:1013–1022.

Sorra KE, Harris KM (1998) Stability in synapse number and size at 2 h

after long-term potentiation in hippocampal area CA1. J Neurosci 18:658–671.
Strange K (1993) Maintenance of cell volume in the central nervous system. Pediatr Nephrol 7:689–697.
Swann JW, Al-Noori S, Jiang M, Lee CL (2000) Spine loss and other dendritic abnormalities in epilepsy. Hippocampus 10:617–625.
Taubenfeld SM, Stevens KA, Pollonini G, Ruggiero J, Alberini CM (2002) Profound molecular changes following hippocampal slice preparation: loss of AMPA receptor subunits and uncoupled mRNA/protein expression. J Neurochem 81:1348–1360.
Volgushev M, Vidyasagar TR, Chistiakova M, Yousef T, Eysel UT (2000a) Membrane properties and spike generation in rat visual cortical cells during reversible cooling. J Physiol 522 (Pt 1):59–76.
Volgushev M, Vidyasagar TR, Chistiakova M, Eysel UT (2000b) Synaptic transmission in the neocortex during reversible cooling. Neuroscience 98:9–22.
Walpoth BH, Walpoth-Aslan BN, Mattle HP, Radanov BP, Schroth G, Schaeffler L, Fischer AP, von Segesser L, Althaus U (1997) Outcome of survivors of accidental deep hypothermia and circulatory arrest treated with extracorporeal blood warming. N Engl J Med 337:1500–1505.
Weisenberg RC, Deery WJ (1981) The mechanism of calcium-induced microtubule disassembly. Biochem Biophys Res Commun 102: 924–931.
Wenzel J, Otani S, Desmond NL, Levy WB (1994) Rapid development of somatic spines in stratum granulosum of the adult hippocampus in vitro. Brain Res 656:127–134.
Zhou Q, Abe H, Nowak TS Jr (1995) Immunocytochemical and in situ hybridization approaches to the optimization of brain slice preparations. J Neurosci Methods 59:85–92.
Ziv NE, Smith SJ (1996) Evidence for a role of dendritic filopodia in synaptogenesis and spine formation. Neuron 17:91–102.

(Accepted 27 April 2004)